

Non-uniform electron density estimation based on electromagnetic wave attenuation in plasma

Zhaoying Wang(王召迎), Lixin Guo(郭立新), Maixia Fu(付麦霞), Shaoshuai Guo(郭韶帅), and Yinsheng Li(李寅生)

Citation: Chin. Phys. B, 2025, 34 (**1**): 015201. DOI: 10.1088/1674-1056/ad9454

What follows is a list of articles you may be interested in

Discharge mode and particle transport in radio frequency capacitively coupled Ar/O_2 plasma discharges

Zhuo-Yao Gao(高卓瑶), Wan Dong(董婉), Chong-Biao Tian(田崇彪), Xing-Zhao Jiang(蒋星照), Zhong-Ling Dai(戴忠玲), and Yuan-Hong Song(宋远红)

Chin. Phys. B, 2024, 33 (**9**): 095203. DOI: 10.1088/1674-1056/ad5d65

Characteristics of the electromagnetic wave propagation in magnetized plasma sheath and practical method for blackout mitigation

Xiang Wu(吴翔), Jiahui Zhang(张珈珲), Guoxiang Dong(董果香), and Lei Shi(石磊)

Chin. Phys. B, 2024, 33 (**5**): 055201. DOI: 10.1088/1674-1056/ad24d4

Analysis of electromagnetic pulses generated from ultrashort laser irradiation of solid targets at CLAPA

Yi-Lin Xu(徐毅麟), Dong-Yu Li(李东彧), Ya-Dong Xia(夏亚东), Si-Yuan Zhang(张思源), Min-Jian Wu(吴旻剑), Tong Yang(杨童), Jun-Gao Zhu(朱军高), Hao Cheng(程浩), Chuan-Ke Wang(王传珂), Chen Lin(林晨), Ting-Shuai Li(李廷帅), and Xue-Qing Yan(颜学庆)

Chin. Phys. B, 2022, 31 (**2**): 025205. DOI: 10.1088/1674-1056/ac3735

Plasma characteristics and broadband electromagnetic wave absorption in argon and helium capacitively coupled plasma

Wen-Chong Ouyang(欧阳文冲), Qi Liu(刘琦), Tao Jin(金涛), and Zheng-Wei Wu(吴征威)

Chin. Phys. B, 2021, 30 (**9**): 095203. DOI: 10.1088/1674-1056/abeb0d

Attenuation characteristics of obliquely incident electromagnetic wave in weakly ionized dusty plasma based on modified Bhatnagar-Gross-Krook collision model

Zhaoying Wang(王召迎), Lixin Guo(郭立新), and Jiangting Li(李江挺)

Chin. Phys. B, 2021, 30 (**4**): 045203. DOI: 10.1088/1674-1056/abe230

Non-uniform electron density estimation based on electromagnetic wave attenuation in plasma

Zhaoying Wang(王召迎)[1,2,†], Lixin Guo(郭立新)[3,‡], Maixia Fu(付麦霞)[1,2], Shaoshuai Guo(郭韶帅)[1,2], and Yinsheng Li(李寅生)[1,2]

[1] *Key Laboratory of Grain Information Processing and Control (Henan University of Technology), Ministry of Education, Zhengzhou* 450001, *China*
[2] *College of Information Science and Engineering, Henan University of Technology, Zhengzhou* 450001, *China*
[3] *School of Physics, Xidian University, Xi'an* 710071, *China*

(Received 17 June 2024; revised manuscript received 5 November 2024; accepted manuscript online 19 November 2024)

The surface of a high-speed vehicle reentering the atmosphere is surrounded by plasma sheath. Due to the influence of the inhomogeneous flow field around the vehicle, understanding the electromagnetic properties of the plasma sheath can be challenging. Obtaining the electron density of the plasma sheath is crucial for understanding and achieving plasma stealth of vehicles. In this work, the relationship between electromagnetic wave attenuation and electron density is deduced theoretically. The attenuation distribution along the propagation path is found to be proportional to the integral of the plasma electron density. This result is used to predict the electron density profile. Furthermore, the average electron density is obtained using a back-propagation neural network algorithm. Finally, the spatial distribution of the electron density can be determined from the average electron density and the normalized derivative of attenuation with respect to the propagation depth. Compared to traditional probe measurement methods, the proposed approach not only improves efficiency but also preserves the integrity of the plasma environment.

Keywords: attenuation, electromagnetic propagation, plasma, electron density

PACS: 52.40.Kh, 94.30.Tz, 98.58.Ay, 42.25.Dd

DOI: 10.1088/1674-1056/ad9454 **CSTR:** 32038.14.CPB.ad9454

1. Introduction

When a high-speed vehicle returns to the atmosphere, its surface experiences friction with the surrounding air, resulting in the formation of high-temperature charged particles around the aircraft. The material, known as the "plasma sheath",[1–5] contains a significant number of free electrons, ions, and neutral molecules that attenuate and interfere with electromagnetic waves, affecting the quality of ground detection and communication. The phenomenon of "blackout"[6,7] during reentry communications is a longstanding problem for significantly impacting real-time tracking, location navigation, and information transmission.

Extensive research over the last century has sought to understand the influence of plasma on electromagnetic waves, yielding numerous results on the propagation and scattering characteristics of electromagnetic waves in various forms of plasma, including uniform, non-uniform, magnetized, non-magnetized, and time-varying plasmas.[8–12] However, many studies have traditionally relied on assumptions about electron density distribution that may not accurately reflect the complex plasma environment. Since electron density distribution directly affects the propagation and scattering characteristics of electromagnetic waves, accurately estimating plasma sheath parameters is crucial for predicting plasma distribution in realistic settings and providing theoretical guidance for radar detection and stealth technology.

Currently, various theoretical models and diagnostic techniques exist for plasma parameters analysis, including methods based on Langmuir probes,[13] microwaves,[14] laser interference,[15] and spectroscopy.[16] The probe method achieves high spatial resolution in measuring electron density, but requires the test probe to penetrate the plasma, which can disturb the plasma flow field. Microwave methods measure only the average electron density, not its spatial distribution. Laser interference is suitable for high electron density measurement. While spectroscopy involves complex data processing and offers relatively low diagnostic accuracy. Statom[17] provided a method for calculating spatial plasma parameters using an imaginary index of the refraction matching algorithm with a tolerance based on the measured attenuation. Wei *et al.*[18] employed convolutional neural network (CNN) techniques to solve the full-wave inverse scattering problem. Li *et al.*[19] developed a novel method combining deep neural network architecture with iterative method for nonlinear electromagnetic wave inverse scattering. Zhang *et al.*[20] proposed multiple regression and artificial neural network methods to address multiple plasma parameter inversion problems, estimating inhomogeneous plasma parameters using a fully con-

†Corresponding author. E-mail: zywang921@163.com
‡Corresponding author. E-mail: lxguo@xidian.edu.cn

© 2025 Chinese Physical Society and IOP Publishing Ltd. All rights, including for text and data mining, AI training, and similar technologies, are reserved.

nected artificial neural network.

In this study, we theoretically derive the relationship between electromagnetic wave attenuation and electron density. By calculating the derivative of attenuation with respect to the propagation depth, we obtain the electron density profile in plasma. This result, combined with the average electron density predicted by back-propagation (BP) neural network method, allows us to predict the spatial distribution of electron density throughout the entire plasma. A schematic diagram of the proposed method is shown in Fig. 1.

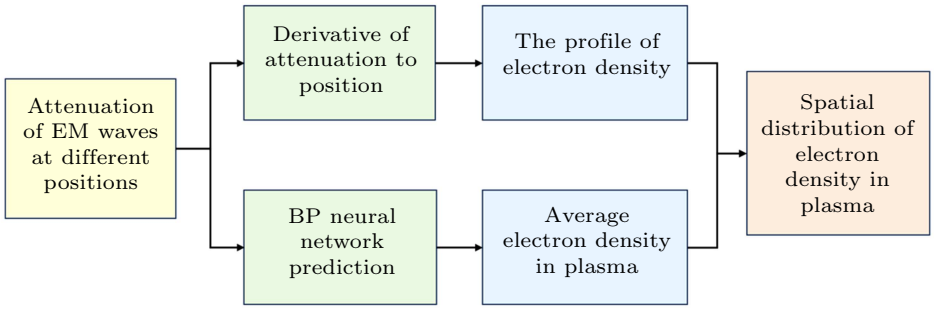


Fig. 1. Schematic diagram of theoretical framework.

The structure of this paper is as follows. Section 2 is the derivation of theoretical formula to clarifying the relationship between the attenuation and the electron density. Section 3 investigates the electron density profile. Section 4 uses the BP neural network to predict the average electron density of the plasma and combines this result with the electron density profile to obtain the spatial distribution of electron density throughout the entire plasma. Section 5 provides a brief summary of the paper.

2. Theoretical derivation

The amplitude and phase changes of electromagnetic wave in plasma depend on the propagation vector. The propagation constant is related to the plasma frequency, defined as follows:[21]

$$\omega_{\mathrm{p}} = \left(n_{\mathrm{e}} \cdot e^2 / m_{\mathrm{e}} \varepsilon_0\right)^{1/2}, \tag{1}$$

where n_{e}, e, m_{e}, and ε_0 are electron density in plasma, electron charge, electron mass, and the permittivity in vacuum, respectively. The dielectric constant of plasma is[2,22–24]

$$\varepsilon = \varepsilon_0 \left[1 - \frac{\omega_{\mathrm{p}}^2}{\omega^2 + \nu^2} + \frac{\nu}{\mathrm{j}\omega} \cdot \frac{\omega_{\mathrm{p}}^2}{\omega^2 + \nu^2}\right], \tag{2}$$

where ν and ω refer to the collision frequency in plasma and the incident frequency.

In isotropic and unmagnetized plasma, Maxwell's equations can be written as

$$\nabla \times \boldsymbol{E} = -\mu_0 \frac{\partial \boldsymbol{H}}{\partial t}, \tag{3}$$

$$\nabla \cdot \boldsymbol{D} = 0, \tag{4}$$

$$\nabla \times \boldsymbol{H} = \varepsilon \frac{\partial \boldsymbol{E}}{\partial t} + \sigma \boldsymbol{E}, \tag{5}$$

$$\nabla \cdot \boldsymbol{H} = 0, \tag{6}$$

where $\boldsymbol{E}$, $\boldsymbol{H}$, $\boldsymbol{D}$, μ_0, and σ are electric field, magnetic field, and electric displacement vector, permeability in vacuum, and conductivity, respectively.

The wave equations of the electric field can be obtained from the above Maxwell equations

$$\nabla^2 \boldsymbol{E} - \mu_0 \varepsilon \frac{\partial^2 \boldsymbol{E}}{\partial t^2} = 0. \tag{7}$$

The effective collision between electrons, neutral molecules, and positive ions is dominant. The general plane wave solution of the electric field wave equation can be expressed as $\boldsymbol{E} = \boldsymbol{E}_0 \exp(-\mathrm{j}(\omega t - \boldsymbol{k} \cdot \boldsymbol{x}))$. For the isotropic medium, the propagation constant is $k = \beta - \mathrm{j}\alpha = \omega(\mu_0 \varepsilon)^{0.5}$, where α and β are the attenuation and phase constants in plasma, respectively. The electromagnetic wave is assumed to propagate along the x axis and the plasma is also distributed along the x axis, as shown in Fig. 2. The expression of the attenuation constant of electromagnetic waves in plasma can be obtained by substituting the expression of dielectric constant into the propagation constant:

$$\alpha = \frac{\omega}{c}\left\{\frac{1}{2}\left[-\left(1 - \frac{\omega_{\mathrm{p}}^2}{\omega^2 + \nu^2}\right) + \sqrt{\left(1 - \frac{\omega_{\mathrm{p}}^2}{\omega^2 + \nu^2}\right)^2 + \left(\frac{\nu}{\omega}\frac{\omega_{\mathrm{p}}^2}{\omega^2 + \nu^2}\right)^2}\right]\right\}^{1/2}. \tag{8}$$

After the electromagnetic wave is passed through the plasma of thickness L, the electric field becomes

$$E = E_0 \exp\left[-\alpha L + \mathrm{j}(\omega t - \beta L)\right]. \tag{9}$$

Thus, the total attenuation of electromagnetic wave in non-uniform plasma is given by

$$A = 20 \log_{10} \frac{|E|}{|E_0|} = 8.68 \int_0^L \alpha(x)\,\mathrm{d}x$$

$$= 8.68\int_0^L \frac{\omega}{c}\left\{\frac{1}{2}\left[-\left(1-\frac{\omega_p^2}{\omega^2+\nu^2}\right)+\sqrt{\left(1-\frac{\omega_p^2}{\omega^2+\nu^2}\right)^2+\left(\frac{\nu}{\omega}\cdot\frac{\omega_p^2}{\omega^2+\nu^2}\right)^2}\right]\right\}^{1/2}\mathrm{d}x. \quad (10)$$

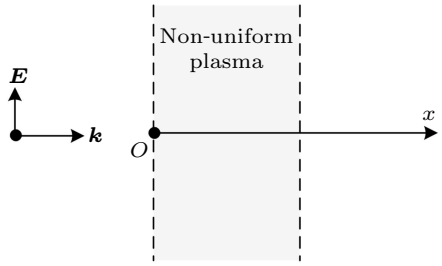


Fig. 2. Illustration of the incident wave and non-uniform plasma.

In order to exploit the electromagnetic wave attenuation at different positions in plasma to determine the electron density, the incident frequency ω of electromagnetic waves must be larger than the characteristic frequency ω_p of the plasma. Based on this, the relationship between the attenuation and the electron density is derived by comparing the differences between the collision frequency and the incident frequency.

If $\omega \gg \nu$, then

$$A = 8.68\int_0^L \frac{\omega}{c}\left\{\frac{1}{2}\left[-1+\sqrt{1+\left(\frac{\nu\omega_p^2}{\omega^3}\right)^2}\right]\right\}^{1/2}\mathrm{d}x. \quad (11)$$

Upon expanding the term $\sqrt{1+\left(\nu\omega_p^2/\omega^3\right)^2}$ in Eq. (11) in a power series and retaining the first two terms, the attenuation can be expressed as

$$A = 8.68\int_0^L \frac{1}{2c}\cdot\frac{\nu\omega_p^2}{\omega^2}\mathrm{d}x. \quad (12)$$

Upon substituting Eq. (1) into Eq. (12), we have

$$A = 8.68\cdot\frac{e^2}{2cm_e\varepsilon_0}\int_0^L \frac{\nu n_e}{\omega^2}\mathrm{d}x. \quad (13)$$

According to Eq. (13), the attenuation is proportional to the integral of the electron density, and thus the derivative of the attenuation with respect to the propagation depth is proportional to the electron density: $\partial A/\partial x \propto \nu n_e/\omega^2$.

If $\omega \ll \nu$, then

$$A = 8.68\int_0^L \frac{\omega}{c}\left\{\frac{1}{2}\left[-1+\sqrt{1+\left(\frac{\omega_p^2}{\omega\nu}\right)^2}\right]\right\}^{1/2}\mathrm{d}x. \quad (14)$$

Upon expanding $\sqrt{1+\left(\omega_p^2/\omega\nu\right)^2}$ to the second order and substituting into Eq. (14), the attenuation is given by

$$A = 8.68\int_0^L \frac{1}{2c}\cdot\frac{\omega_p^2}{\nu}\mathrm{d}x. \quad (15)$$

By substituting Eq. (1) into Eq. (15), we have

$$A = 8.68\cdot\frac{e^2}{2cm_e\varepsilon_0}\int_0^L \frac{n_e}{\nu}\mathrm{d}x. \quad (16)$$

As shown in Eq. (16), the attenuation is proportional to the integral of the electron density. Therefore, the relationship between the attenuation and the electron density remains unchanged. It can be obtained: $\partial A/\partial x \propto n_e/\nu$. Consequently, in both cases, the the electron density profile can be accessed by calculating the derivative of attenuation with respect to position. This forms the basis of the following discussions.

3. Simulation of electron density profile

3.1. The influence of plasma parameters on electromagnetic wave attenuation

The results presented in Fig. 3 are obtained from Eq. (10) using an incident wave frequency $f = 10$ GHz. As shown in Fig. 3(a), the attenuation of electromagnetic wave initially increases and then decreases with the increase of collision frequency. This is because a larger collision frequency results in a greater collision probability between electrons and neutral particles, thereby increasing the energy transmitted to neutral particles. However, with a further increase in collision frequency, electrons are accelerated by the electric field for a short duration before colliding with neutral particles, leading to reduced energy absorption from the electric field and consequently decreasing electromagnetic wave attenuation. In general, regardless of the relationship between the collision frequency and the incident frequency, the attenuation of electromagnetic waves through plasma is proportional to the plasma thickness.

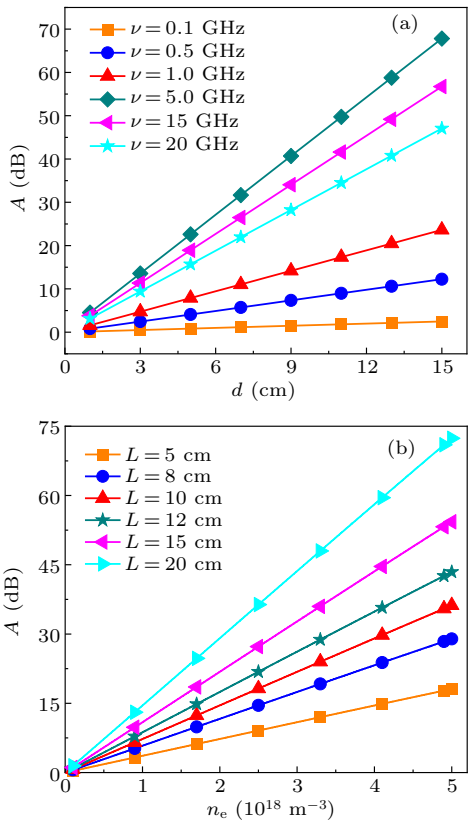


Fig. 3. The influence of different parameters on attenuation: (a) different collision frequencies (ν) and (b) different plasma thicknesses (L).

At fixed collision frequency, the attenuation is positively correlated with the electron density across different plasma thickness, as shown in Fig. 3(b). For a given plasma thickness, a larger electron density corresponds to a greater electromagnetic energy attenuation. This is because increased thickness results in longer interaction time between electromagnetic waves and plasma. Furthermore, the attenuation of electromagnetic wave through plasma is proportional to the line integral of electron density, as demonstrated in Eqs. (13) and (16). These findings corroborate the theoretical analysis presented in Section 2.

3.2. Estimating electron density profile using derivative of attenuation with respect to the position

Figure 4 displays the predicted results using four types of electron density distributions: linear, parabolic, Epstein, and Gaussian. The collision frequency $\nu = 20$ GHz, and incident wave frequency $f = 10$ GHz were adopted in simulation. For clarity of comparisons, all results were normalized. The predicted values align well with the assigned ones, confirming the validity of our approach.

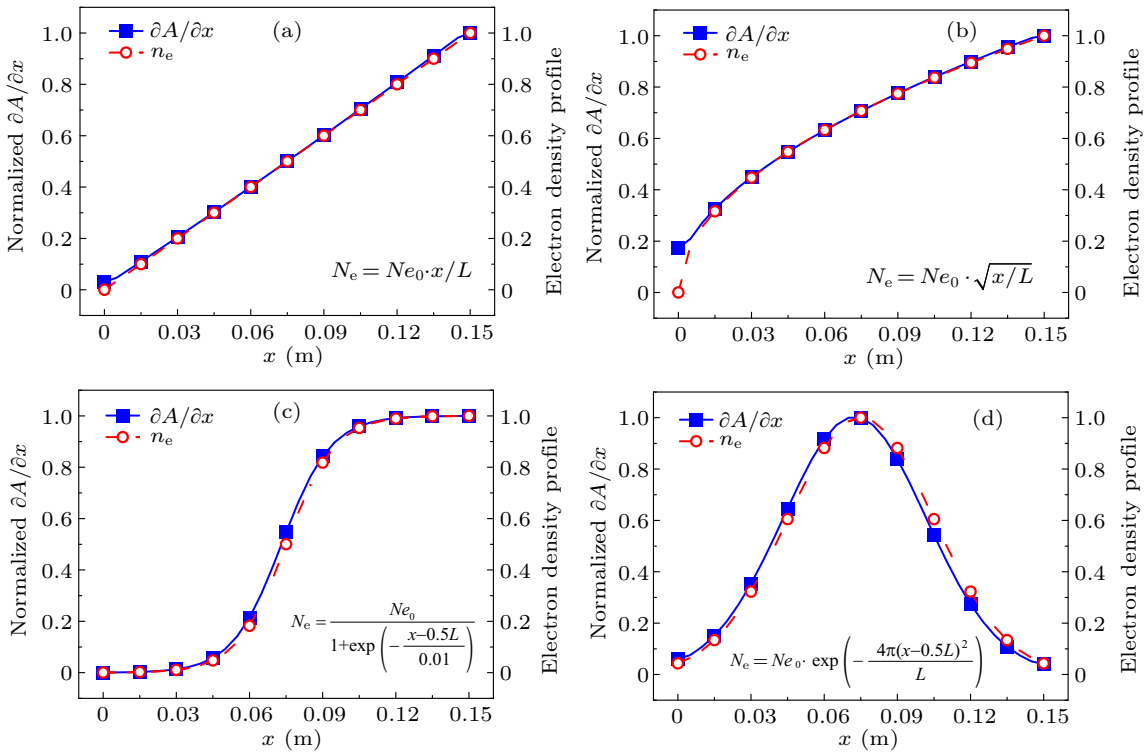


Fig. 4. Estimation of electron density profiles based on different spatial distribution types: (a) linear, (b) parabolic, (c) Epstein, and (d) Gaussian.

However, this method can only estimate the electron density profile in plasma and discriminate the distribution type, and cannot determine the order of magnitude of the electron density. Therefore, it is challenging to achieve complete characterization of the electron density without specific electron density values, and quantitative assessment of electron density remains necessary.

4. Estimation of spatially non-uniform electron density in plasma

4.1. Relationship between electromagnetic wave attenuation and average electron density

The electromagnetic wave attenuations under the two conditions: (i) different electron density distribution type and (ii) the uniform distribution with the electron density equal to the average value in Eq. (1), were investigated with the parameters: collision frequency $\nu = 20$ GHz, plasma thickness $d = 0.2$ m, and incident wave frequency $f = 10$ GHz. The comparisons of the attenuation results are presented in Table 1.

Table 1. Comparisons of the attenuation (A) under different electron density distribution types and the corresponding uniform distribution with average electron density (A_{ave}).

Distribution types	A (dB)	Average electron density (m^{-3})	A_{ave} (dB)
Uniform	5.9250	1.00×10^{17}	5.9250
Linear	2.9547	5.00×10^{16}	2.9507
Parabolic	3.9369	6.66×10^{16}	3.9342
Gaussian	2.9065	4.92×10^{16}	2.9013
Epstein	2.9602	5.00×10^{16}	2.9507

Table 1 presents the attenuation results of electromagnetic waves passing through plasma with different spatial distribution types of electron density and their corresponding average electron densities. The results show that the attenuation of electromagnetic wave in these scenarios is almost consistent,

allowing for the estimation of the average electron density of plasma at a given thickness by measuring the attenuation value of the electromagnetic wave.

To further illustrate this, we analyze the attenuation results of electromagnetic waves across different spatial distribution types with the corresponding average electron densities. Here, the average electron density ($\bar{n}_e$) set to 1.0×10^{16} m^{-3}, 5.0×10^{16} m^{-3}, 1.0×10^{17} m^{-3}, 5.0×10^{17} m^{-3}, and 1.0×10^{18} m^{-3}, respectively. As shown in Fig. 5, the attenuation of the electromagnetic wave increases with the average electron density for all the aforementioned distribution types. This is results from increased electron density enhances scattering between electrons and neutral particles. For a given average electron density, the attenuation of electromagnetic wave exhibits similar values for different spatial distribution types. This indicates that estimating average electron density from attenuation does not effectively distinguish the spatial distribution features of the electron density. In such cases, the spatial distribution of electron density in plasma can be obtained by evaluating the average electron density value and combining it with the obtained electron density profile.

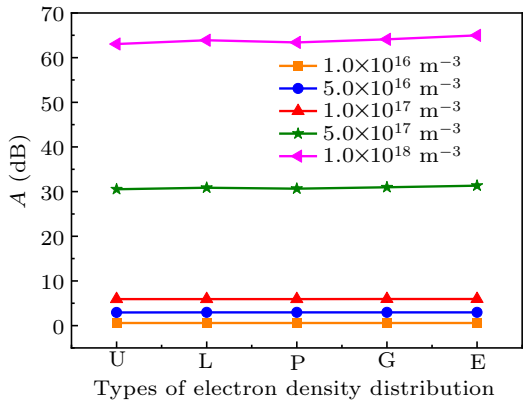


Fig. 5. The attenuation as a function of average electron density under different spatial distribution types: U: uniform, L: linear, P: parabolic, G: Gaussian, E: Epstein.

4.2. Average electron density predicted by BP neural network method

The BP neural network, known for its robust theoretical foundation and strong learning ability, has been widely used.[19,25–30] As an intelligent information processing method, the BP neural network does not require predefined mathematical expressions between input and output. It learns from the provided data to identify implicit patterns, allowing for quick and accurate output of the desired results based on given input. Given the effectiveness and accuracy of BP neural networks in predicting nonlinear relationships,[28–30] this method was adopted to predict average electron density in plasma.

Table 2 shows the average electron density of the plasma layer as predicted by the BP neural network method. The relative error compared to the expected value of the average electron density is kepted within 6%, indicating the high accuracy of this method in predicting the average electron density value.

Table 2. Predicted and expected electron density, and relative errors based on the BP neural network method.

Distribution type	Predicted values (m^{-3})	Expected values (m^{-3})	Relative errors
Linear	5.27×10^{17}	5.00×10^{17}	0.0543
Parabolic	6.79×10^{17}	6.60×10^{17}	0.0284
Epstein	5.23×10^{17}	5.00×10^{17}	0.0460
Gaussian	4.96×10^{17}	4.79×10^{17}	0.0354

4.3. Estimation of spatial distribution of electron density in plasma

The profile of electron density can be obtained as mentioned above. The spatial distribution of electron density across the entire plasma can be determined via accurately obtaining the electron density value at a given position. Conversely, attenuation measurements provide the mean electron density within a specific region. Therefore, the average electron density value obtained with different distributions can be used to predict the spatial distribution of the electron density. Considerate the accuracy of the BP neural networks in nonlinear relation prediction, this method was adopted to predict the average electron density in plasma.

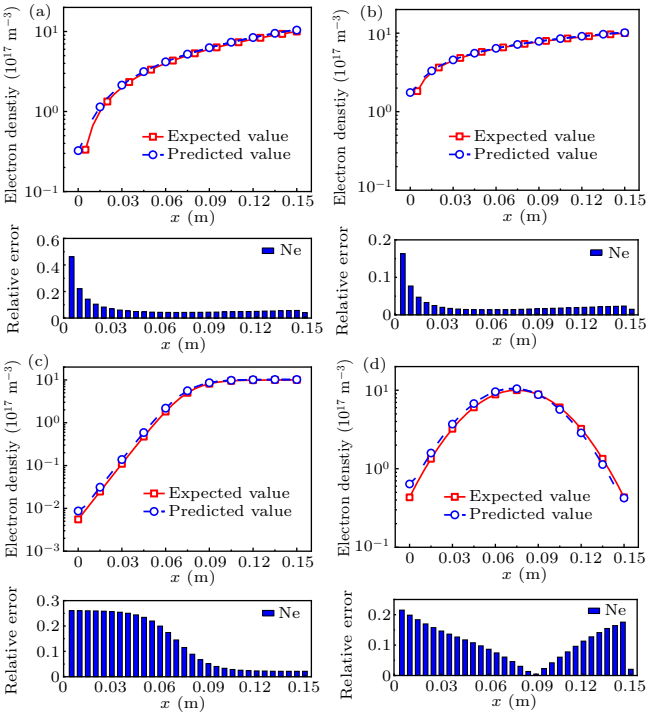


Fig. 6. Estimation of different electron density distributions (the corresponding relative errors in the bottom panels): (a) linear distribution, (b) parabolic distribution, (c) Epstein distribution, (d) Gaussian distribution.

Figure 6 presents the predicted spatial distribution of electron density under different plasma flow fields as modeled by our method. The predicted curves closely match the expected outcomes, with a smaller relative error observed at higher electron densities. This is because lower electron densities allow

electromagnetic waves of a fixed incident frequency to penetrate more effectively. Consequently, this leads to most of the electromagnetic waves passing through the plasma with reduced attenuation, which can slightly decrease the prediction accuracy for electron density.

5. Conclusion

In this study, the theoretical relationship between electromagnetic wave attenuation and electron density in plasma was derived. The attenuation pattern along the propagation path is directly proportional to the integral of the plasma electron density. Using this relationship, the normalized derivative of attenuation was calculated from results at different positions and compared with the normalized set electron densities. These comparisons demonstrate that the proposed method effectively captures the spatial profile of electron density. Subsequently, a BP neural network was utilized to predict the average electron density. Combining the average electron density with the trend of electron density distribution in the plasma, we can obtain the spatial distribution of electron density throughout the plasma. The estimated distributions show a strong agreement with the expected profiles. This work offers a methodology to improve transmission models and design appreciate electron density reconstructions.

Acknowledgements

Project supported by the Natural Science Foundation of Henan Province, China (Grant No. 242300420634), the Cultivative Plan of Henan University of Technology (Grant No. 2024PYJH035), the Research Foundation for Advanced Talents of Henan University of Technology (Grant Nos. 2022BS067 and 2022BS068), the National Natural Science Foundation of China (Grant No. 62301211), the Key Research and Development and Promotion Special Project (Science and Technology Research) in Henan Province, China (Grant No. 232102211068), and the Innovative Funds Plan of Henan University of Technology (Grant No. 2022ZKCJ15).

References

[1] Liu J F, Xi X L, Wan G B and Wang L L 2011 *IEEE Trans. Plasma Sci.* **39** 852
[2] Bai B W, Li X P, Liu Y M, Xu J, Shi L and Xie K 2014 *IEEE Trans. Plasma Sci.* **42** 3365
[3] Chen W, Guo L X and Li J T 2017 *Phys. Plasmas* **24** 042102
[4] Yao B, Shi L, Li X, Wei H and Liu Y 2022 *IEEE Trans. Plasma Sci.* **50** 2430
[5] Guo S S, Xie K, Xu H, Fu M X and Niu Y Y 2023 *Plasma Sci. Technol.* **25** 065401
[6] Liu Z W, Bao W M, Li X P, Liu D L and Bai B W 2015 *IEEE Trans. Plasma Sci.* **43** 3147
[7] Wang Z Y, Guo L X and Li J T 2021 *Plasma Sci. Technol.* **23** 075001
[8] Joo Hwa L and Kalluri D K 1999 *IEEE Trans. Antenn. Propag.* **47** 1146
[9] Laroussi M and Roth J R 1993 *IEEE Trans. Plasma Sci.* **21** 366
[10] Chen W, Yang L X, Huang Z X and Guo L X 2019 *J. Quantum Spectrosc Rad. Transf.* **232** 66
[11] Wang Z Y, Guo L X, Dan L and Li J T 2019 *IEEE Trans. Plasma Sci.* **47** 3978
[12] Chen W, Guo L X, Li J T and Liu S H 2016 *IEEE Trans. Plasma Sci.* **44** 3235
[13] Ryan P J, Bradley J W and Bowden M D 2019 *Phys. Plasmas* **26** 040702
[14] Shneider M N and Miles R B 2005 *J. Appl. Phys.* **98** 033301
[15] Garland J M, Tauscher G, Bohlen S, Boyle G J, D'Arcy R, Goldberg L, Poder K, Schaper L, Schmidt B and Osterhoff J 2021 *Rev. Sci. Instrum.* **92** 013505
[16] Berchtikou A, Lavoie J, Poenariu V, Saoudi B, Kashyap R and Wertheimer M R 2011 *IEEE Trans. Dielect. El. In.* **18** 24
[17] Statom T K 2018 *IEEE Trans. Plasma Sci.* **46** 494
[18] Wei Z and Chen X D 2019 *IEEE Trans. Geosci. Remote.* **57** 1849
[19] Li L L, Wang L G, Teixeira F L, Liu C, Nehorai A and Cui T J 2019 *IEEE Trans. Antenn. Propag.* **67** 1819
[20] Zhang Y Y, Fu H Y and Sui Y 2020 *IEEE Trans. Plasma Sci.* **48** 2143
[21] Guo B and Wang X G 2005 *Phys. Plasmas* **12** 084506
[22] Du Y X, Li C L and Qin L 2017 *IEEE Trans. Plasma Sci.* **45** 3182
[23] Guo X M, Li H Y, Bo Y, Chen W, Yang L X, Huang Z X and Wang A Q 2024 *Appl. Comput. Electrom.* **39** 156
[24] Gao Y, Yang M, Xie K, Qiao L, Liu H, Li C, Liu D, Quan L, Wu M and Li X 2024 *Phys. Plasmas* **31** 023505
[25] Buscema M 1998 *Subst Use Misuse* **33** 233
[26] Lu Q, Yang R, Zhong M and Wang Y 2020 *IEEE Trans. Instrum. Meas.* **69** 1585
[27] Shi S, Zhou K, Zhao J, Mukherjee S and Zhuang P 2022 *Phys. Rev. D* **105** 014017
[28] Cui K and Jing X 2019 *Neural Comput. Appl.* **31** 8205
[29] Wang D, Luo H, Grunder O, Lin Y and Guo H 2017 *Appl. Energy* **190** 390
[30] Sun W and Huang C 2020 *J. Clean Prod.* **243** 118671